ORIGINAL ARTICLE

MOLECULAR ECOLOGY WILEY

Host genotype and microbiome associations in co-occurring clonal and non-clonal kelp, *Ecklonia radiata*

Sebastian Vadillo Gonzalez[1,2] | Sofie Vranken[3] | Melinda A. Coleman[3,4] | Thomas Wernberg[3,5] | Peter D. Steinberg[2,6] | Ezequiel M. Marzinelli[1,2,7]

[1]The University of Sydney, School of Life and Environmental Sciences, Sydney, New South Wales, Australia

[2]Sydney Institute of Marine Science, Mosman, New South Wales, Australia

[3]UWA Oceans Institute & School of Biological Sciences, University of Western Australia, Crowley, Western Australia, Australia

[4]New South Wales Fisheries, Department of Primary Industries, National Marine Science Centre, Coffs Harbour, New South Wales, Australia

[5]Institute of Marine Research, Floedevigen Research Station, His, Norway

[6]School of Biological, Earth and Environmental Sciences, University of New South Wales, Sydney, New South Wales, Australia

[7]Singapore Centre for Environmental Life Sciences Engineering, Nanyang Technological University, Singapore City, Singapore

Correspondence

Sebastian Vadillo Gonzalez, Sydney Institute of Marine Science, The University of Sydney, School of Life and Environmental Sciences, Life, Earth and Environmental Sciences Building (LEES, F22), City Rd & Eastern Ave, Camperdown, NSW 2006, Australia.
Email: sebastian.vadillo@sims.org.au

Abstract

A fundamental question in holobiont biology is the extent to which microbiomes are determined by host characteristics regulated by their genotype. Studies on the interactions of host genotype and microbiomes are emerging but disentangling the role that host genotype has in shaping microbiomes remains challenging in natural settings. Host genotypes tend to be segregated in space and affected by different environments. Here we overcome this challenge by studying an unusual situation where host asexual (5 clonal lineages) and sexual genotypes (15 non-clonal lineages) of the same species co-occur under the same environment. This allowed us to partition the influence of morphological traits and genotype in shaping host-associated bacterial communities. Lamina-associated bacteria of co-occurring kelp sexual non-clonal (*Ecklonia radiata*) and asexual clonal (*E. brevipes*) morphs were compared to test whether host genotype influences microbiomes beyond morphology. Similarity of bacterial composition and predicted functions were evaluated among individuals within a single clonal genotype or among non-clonal genotypes of each morph. Higher similarity in bacterial composition and inferred functions were found among identical clones of *E. brevipes* compared to other clonal genotypes or unique non-clonal *E. radiata* genotypes. Additionally, bacterial diversity and composition differed significantly between the two morphs and were related with one morphological trait in *E. brevipes* (haptera). Thus, factors regulated by the host genotype (e.g. secondary metabolite production) likely drive differences in microbial communities between morphs. The strong association of genotype and microbiome found here highlights the importance of genetic relatedness of hosts in determining variability in their bacterial symbionts.

KEYWORDS
Ecklonia, genotype–microbiome interaction, holobiont, host specificity, kelp, morphology

-WILEY |

1 | INTRODUCTION

Recent research has provided strong evidence for the importance of the relationships between host organisms and their associated microbiota in forming functional ecological units or 'holobionts' (Dittami et al., 2021). Holobionts are composed of multiple microbial communities that interact with the host and can determine and regulate multiple processes that support the host's performance, development, survival, and resilience to changing environments and different stressors (Egan et al., 2013; DeWeese & Osborne, 2021). Holobionts have been studied in multiple models from single-cell interactions (Sallinger et al., 2021) to larger and more complex systems that include invertebrates, vertebrates and plants (Rosenberg & Zilber-Rosenberg, 2014). These studies reveal that symbionts play a significant role in resource acquisition, health, pathogen regulation and fitness of the host, while hosts provide microbiomes with similar benefits (Fietz et al., 2018).

Changing environmental conditions surrounding holobionts can determine much of the variability observed in host and their associated microbiomes (Phelps et al., 2021 and Whipps et al., 2008). However, intraspecific genotypic differences can determine phenotypical variation in hosts (Whipps et al., 2008), which, in turn, may also lead to changes in the associated microbes and the functional interactions that exist between them (Coyte et al., 2015). While the complexity and intraspecific variability of holobionts is determined not only by the environment, but also by processes that are dependent at least in part on the host's genetic makeup, these factors are often difficult to disentangle. Morphological variation between individuals is, to some extent, influenced by the host genotype, but other phenotypic traits that often have a strong genetic component, such as the release of waste compounds, secondary metabolites or the host's immune response, may have a stronger effect on the microbiome (Coyte et al., 2015; Griffiths et al., 2019). Indeed, microbiomes regulated by these traits are typically more similar between individuals with higher genetic relatedness (Engel et al., 2020; Selber-Hnatiw et al., 2020). For instance, although human gut microbiomes can be highly variable, with each individual person having a unique microbiota (Rosenberg & Zilber-Rosenberg, 2014), there is a higher microbiome similarity between related individuals such as identical twins (Goodrich et al., 2016; Selber-Hnatiw et al., 2020) and similar trends have been observed for other species (Benson et al., 2010; Fietz et al., 2018; Griffiths et al., 2018; Pearce et al., 2017; Uren Webster et al., 2018). In marine systems, corals can directly influence the abundance of their microbial symbionts through upregulating the expression of specific genes (e.g. iron sequestration and oxygen stress response) and this response has been found to have intraspecific variability and related to how genetically similar the coral colonies are (Parkinson et al., 2015). Multiple other recent examples in corals have also demonstrated the influence of host genotype on the associated microbial communities (*Acropora tenuis*, Glasl et al., 2019; and *Millepora* sp., Dubé et al., 2021). Similarly, a higher genetic relatedness among sponges of the same species has

been seen to translate into a higher similarity of their associated microbiome (Griffiths et al., 2019). Kelps (large brown macroalgae) are dominant marine habitat-formers that underpin coastal biodiversity. Kelp health and function are affected by changes in their microbiome (e.g. Marzinelli et al., 2015; Qiu et al., 2019), but we have little information about the relationship between host genetics and their microbiome (Wood et al., 2022). Understanding the link between the host's genotype, phenotype and its microbiome is essential to determine the potential influences of environmental change on natural populations.

Ecklonia radiata is a laminarian kelp that dominates temperate and subtropical rocky reefs across much of the southern hemisphere (Wernberg et al., 2019). Like other kelps, *E. radiata* has a haplodiplontic life cycle that alternates through a haploid gametophyte phase and a diploid sporophyte (Figure 1a). However, vegetative reproduction has also been observed at the sporophyte phase in a different morph of *E. radiata*, named *Ecklonia brevipes*, in restricted populations in Western Australia where both morphs co-occur (Cape Leeuwin; Coleman & Wernberg, 2018, Vranken et al., 2022). Similar modes of vegetative reproduction in *E. radiata* have been observed in other species (e.g. *Ecklonia stolonifera*, Hayashi et al., 2020) through the formation of specialized structures in the sporophyte (e.g. haptera) that eventually create new individuals that are clones of the parent kelp (see Figure 1b, based on Coleman & Wernberg, 2018). These modes of reproduction appear to be fixed with no clones (asexual reproduction) apparent among individuals of the sexual morph and both morphs adopting the same life history as their sporophyte parents in culture (Coleman & Wernberg 2018; Vranken et al., 2022). Large morphological differences exists between both *Ecklonia* morphs, including differences in the size of laminae and the presence of lateral haptera, but the two morphs are still considered to be a single species (Rothman et al., 2015). However, to ease clarity within this study, the denomination of the vegetative morph as *E. brevipes* has been retained.

The difference in genetic make-up between the two morphs and the greater variability in genotype in the sexually non-clonal reproducing vs. asexual clonal morph could be important drivers of the structure and function of their associated microbiomes. In this study, the bacterial communities associated with laminae of these two morphs (i.e. non-clonal *E. radiata* and clonal *E. brevipes*) co-occurring in the same area and with a consistent environment were compared and contrasted between several morphological traits and genotypes, including among individuals within and between morphs and among clones. Specifically, we predicted that bacterial communities would be more similar and less variable among identical clones of *E. brevipes* compared to different unique clonal genotypes of the same morph, which, in turn, would be more similar and less variable than unique non-clonal *E. radiata* genotypes produced exclusively by sexual reproduction (predictions in Figure 2b). The results generated in this study help unravel the potential influence that host genotype can have, beyond differences in morphological traits, on associated microbiomes.
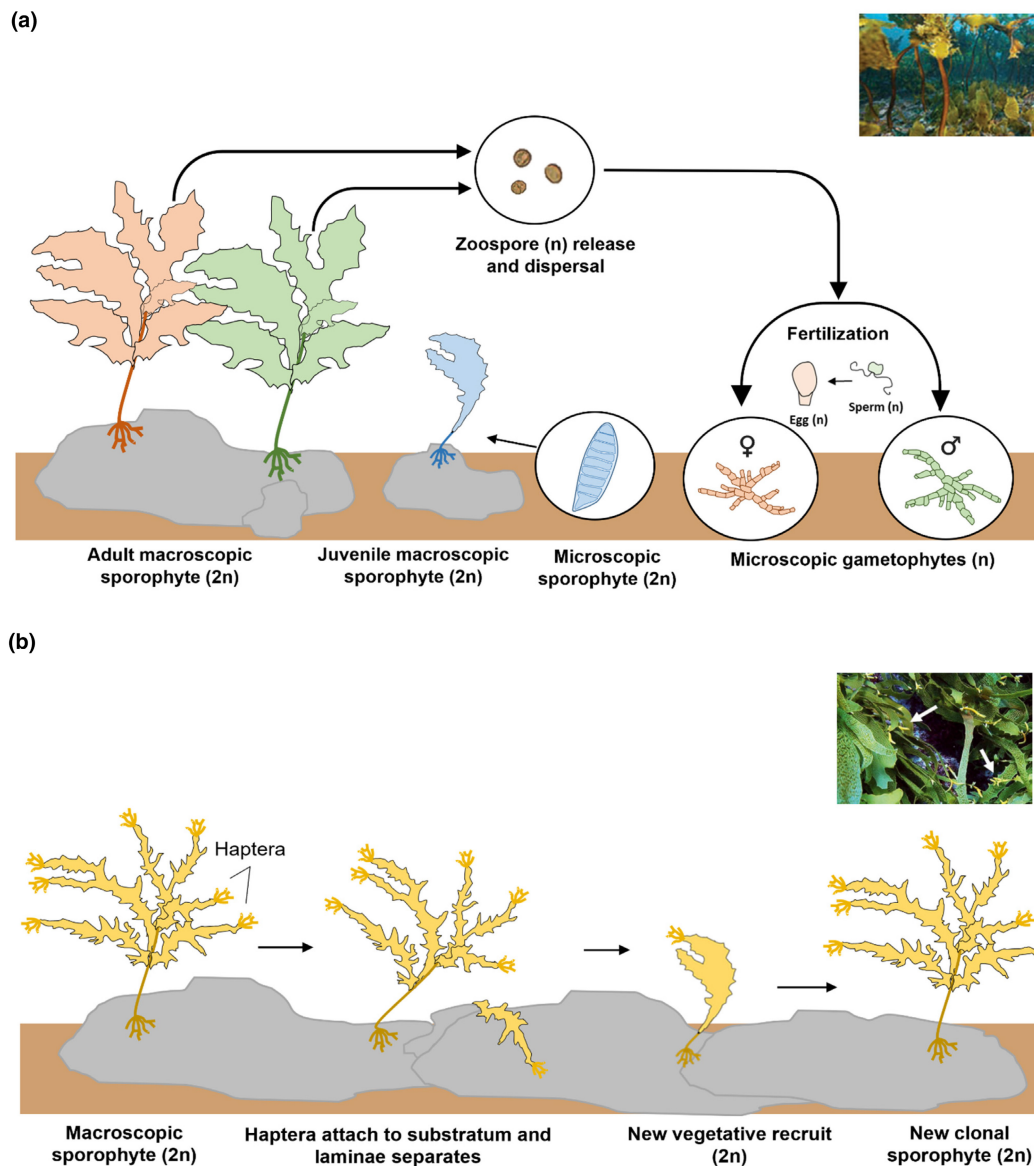
(a)

(b)

FIGURE 1 General description of the reproductive mechanisms in *Ecklonia radiata* including A) sexual reproduction that produces unique genotypes through a haplodiplontic life cycle that alternates through a haploid gametophyte (n) phase and a diploid sporophyte (2n) and B) a vegetative reproduction of the diploid sporophyte (2n) seen only on the *E. brevipes* morph. Different colours of the algae represent distinct genotypes. (a) *E. radiata* sexual reproduction to produce unique genotypes. (b) *E. brevipes* vegetative reproduction to produce clonal genotypes.

2 | MATERIALS AND METHODS

2.1 | Field sampling and morphological measurements

Adult sporophytes (stage 3 cf. Kirkman, 1981) of both morphs (i.e. *E. radiata* and *E. brevipes)* from Hamelin Bay, Western Australia (34°13′48.79″ S; 115°0′52.70″ E) were collected at 11 m depth by SCUBA. While individuals of *E. radiata* occur homogeneously on the reefs, the distribution of *E. brevipes* can be patchy, with patches of *E. brevipes* separated by 5–15 m (Figure 2a). The two morphs are interspersed on many reefs like the one sampled in this study, co-occurring in the same area and under the same

environmental conditions. All samples were collected haphazardly within an area of ~50 m² with individual kelps separated by at least 1 m (Figure 2a). Before collection, 15 individuals of each morph were labelled, and a clean lateral lamina was cut and carefully folded into a clean, labelled zip lock bag for microbial sampling. The surface of these laterals and secondary lamina at mid-thallus were swabbed (5 × 4 cm) for 30 s using a sterile cotton swab before genetic samples were taken (Marzinelli et al., 2015; Qiu et al., 2019). A 'blank' swab, that is handled similarly to other swabs except it was not used to swab kelp, was included to control for potential contamination. Swabs were immediately placed in sterile cryogenic tubes in liquid nitrogen and then stored in a −80°C freezer. All labelled individuals were then taken ashore and
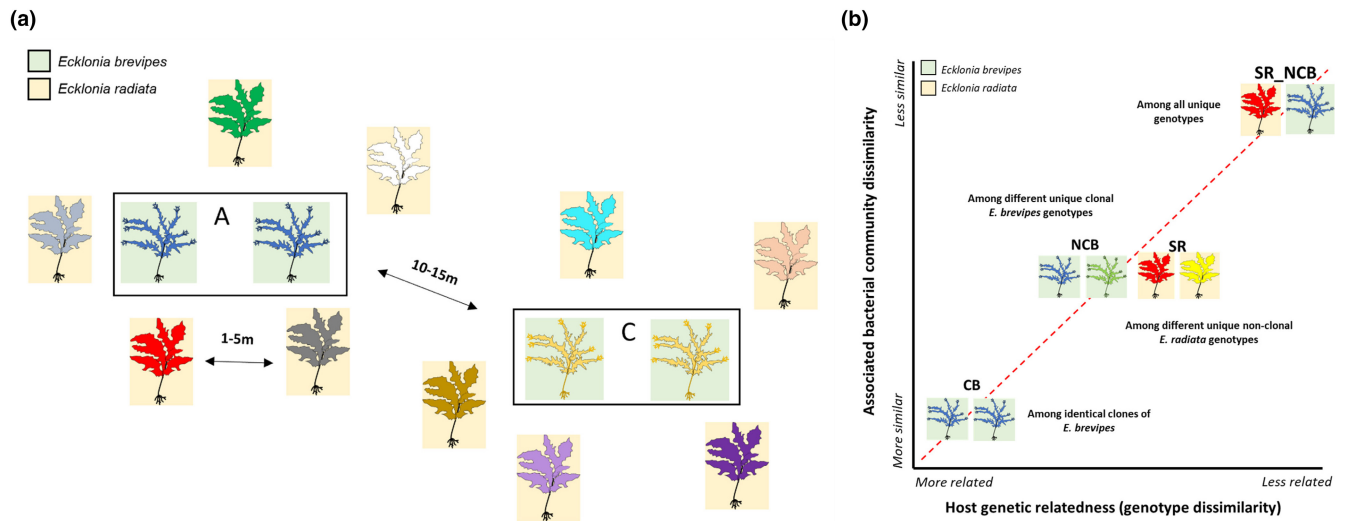
FIGURE 2 Experimental setup and spatial arrangement of co-occurring *Ecklonia* morphs (*E. radiata* and *E. brevipes*) across the experimental area (a) and the predicted outcomes showing that associated bacterial community similarity (i.e. composition and predicted function) is expected to increase as hosts have higher genetic relatedness determined by genotype similarity (b). Different kelp colours represent different genotypes and background (green or yellow) indicates the type of *Ecklonia* morph. Letters and boxes surrounding *E. brevipes* in A represent the same clonal genotype. Distance between algal patches (both morphs fully interspersed art each patch, 10–15 m) and distances between individuals (1–5 m) are also shown. In (b), labels indicate same clonal genotype of *E. brevipes* (CB, based on 4 genotypes); different clones of *E. brevipes* (NCB, 9 genotypes); all individuals of *E. radiata* with unique genotypes (SR, 15 genotypes) and among all genotypes of both morphs (SR_NCB, 24 genotypes). (a) Co-occurring *Ecklonia* morphs in the same experimental area. (b) Predicted outcomes.

for every individual a clean young lateral was also snapped frozen for DNA extraction and genotype description. The remaining sections of the individuals were kept moist and shaded until processed for morphological measurements. In total, 12 morphological measurements were taken (Table S1).

2.2 | Genotype description

In all, 15 *E. brevipes* and 10 *E. radiata* individuals were swabbed for microbial assemblages and then processed for genotype description. DNA extraction and DNA clean-up were performed as in Vranken et al. (2021). Technical replicates were taken from *E. radiata* to be able to distinguish unique and clonal genotypes. Following quality control, ddRAD (double digest restriction associated DNA) libraries were developed as in Vranken et al. (2021). Briefly, 200 ng of DNA per sample was used to prepare ddRAD libraries adjusting the protocol of Severn-Ellis et al. (2020). Following digestion with restriction enzymes *PstI* and *NlaIII* (New England Biolabs [NEB]), the DNA fragments of each individual sample were ligated to a unique barcoded adaptor. Double size selection to retain 250–800 bp fragments was performed with solid-phase reversible immobilization beads (SPRI, AMPure XP; Beckman Coulter). The libraries generated were amplified by polymerase chain reaction (PCR) using Phusion Hot-Start High-Fidelity Master Mix Polymerase (Thermo Fisher Scientific) and purified with SPRI beads. The quality of each library was confirmed using a LabChip GX Touch and the

concentration determined using a Qubit. Equimolar concentrations were pooled per 96 libraries, and each pool was sequenced on one lane of Illumina XTEN at the Kinghorn Centre for Clinical Genomics' Sequencing Facility. SNP calling and filtering were performed as in Vranken et al. (2022). Briefly, Illumina sequencing base calls were converted to FASTQ format using BCL2FASTQ (v2.19). Sequences were further processed for de novo SNPs calling with Stacks (Catchen et al., 2013). Further filtering to retain only high-quality SNPs was performed with VCFTOOLS 0.1.15 (Danecek et al., 2011). All indels, multiallelic sites and all individuals containing >75% missing data were removed. Furthermore, a minimum depth of coverage (DP) of 3 and maximum coverage of 2× mean sequencing depth, maximum missingness of 10% per site, and a minimum allele frequency of 0.02 were required. Only SNPs with maximum heterozygosity of 80% and present in at least 80% of the individuals were included using Stacks (Catchen et al., 2013), resulting in a final dataset of 5597 SNPs with multiple SNPs per RAD locus and 14 *E. brevipes* individuals and 10 *E. radiata* individuals.

Unique genotypes were identified as in Vranken et al. (2022). Briefly, the divergence among samples was estimated as bitwise distance which was calculated with POPPR v 2.8.3 (Kamvar et al., 2014, 2015). The minimum bitwise distance found between technical replicate samples of *E. radiata* ($d = 0.019$) was used as a threshold. All individuals separated by a distance lower than this threshold were considered to belong to the same unique genotype. All *E. radiata* samples were found to be unique genotypes (15 unique non-clonal genotypes). For *E. brevipes*, we found

five genotypes (clonal lineages) containing two individuals each and four genotypes containing one individual (total of 9 clonal genotypes).

2.3 | Microbial sampling and sequencing

Microbial DNA was extracted in random order from each swab using a DNEasy Powersoil Pro kit (Qiagen, Hilden, Germany) following the manufacturer's guidelines. Briefly, genomic DNA is extracted through mechanical and chemical homogenizations that optimize cell lysis and removal of any PCR inhibitors. A silica spin filter membrane is then used to isolate the DNA from the purified lysate which is then eluted in a 10 mM Tris buffer. Isolated DNA extracts were stored in a −20°C freezer until amplification with PCR (Master mix: KAPA HiFi Hot Start Ready-mix (2×), Cat No. KK2602; Roche; 30 cycles) using the primers 341F (5′ -CCTACGGGNGGCWGCAG- 3′) and 805R (5′ -GACTACHVGGGTATCTAATCC- 3′), which target V3-V4 regions of the 16S rRNA gene (Klindworth et al., 2013). No DNA was amplified from the blank (control) swabs. Agarose gel electrophoresis, Nanodrop 1000 and the QUBIT 2.0 Fluorometer (Thermo Fisher Scientific) were used to check the quality and quantity of the amplicons before being sent to the Ramaciotti Centre for Genomics (UNSW) for sequencing via the Illumina MiSeq Platform (2×300 bp run, Reagent Kit v3 600-cycle and 10% PhiX control spike-in). All original amplicon sequences were provided as pair-end demultiplexed FASTQ files by the sequencing centre and were submitted to the NCBI Sequence Read Archive (SRA) database (BioProject accession number: PRJNA891085).

2.4 | Bioinformatics

Raw sequences were received from the sequencing centre as demultiplexed paired-ended sequences per sample (i.e. a forward sequence with direction 5′-3′ and its reverse complementary sequence). Primers present in the sequences were identified and removed by initially deleting ambiguous nucleotide bases (Ns) and then trimming them using the program CUTADAPT *v.3.4.* (Martin, 2011, running within a *conda* environment using PYTHON v.3.9). A quality trimming step was subsequently done, adjusting the maximum expected error to 2 and 6 base pairs in the forward and reverse sequence respectively. Additionally, a maximum truncation length for both paired sequences was decided upon inspection of quality error plots (i.e. truncation at a maximum length of 240 base pairs for both paired sequences) and based on a mean Q score of 20. Any base pairs with a lower Q score of 20 were dropped. Independently of the trimming process, a maximum error rate model was constructed for each paired read using the overall error rate from the sequencing process and ensuring their fit through complementary-base error plots. These error rate models were used to determine exact amplicon sequence variants (ASV) using the core DADA2 algorithm (Callahan et al., 2016) to perform a two-step denoising process (i.e. pseudo-pooling) that enabled a higher detection of rare ASV. All paired-ended sequences were merged into unique ASV, arranged into an abundance by sample table and chimeric sequences removed. An average of 79% of the original raw sequences per sample was kept at the end of the pipeline. These surviving reads were assigned within 6373 ASV and identified taxonomically using a trained version of the prokaryotic SSU taxonomic database SILVA v.138.1 formatted and optimized exclusively for the DADA2 pipeline (Quast et al., 2012). Six taxonomic levels were assigned to each ASV (i.e. kingdom, phylum, class, order, family and genus). ASV identified as chloroplasts, mitochondria and eukaryotes were removed. All steps in the pipeline unless specified were done using R v.3.6. and the package dada2 v. 1.20 (Callahan et al., 2016).

2.5 | Bacterial functional predictions

To better understand the differences in bacterial communities between *Ecklonia* morphs and lineages, functional profiles of these communities were predicted using the software PICRUST2 v.2.4.0 through a whole-genome reconstruction based on the 16S rRNA gene amplicon sequences (i.e. Phylogenetic Investigation of Communities by Reconstruction of Unobserved States; ran within a *conda* environment using PYTHON *v.3.9*; Douglas et al., 2020). Briefly, all unique ASV sequences were aligned and placed into a reference phylogenetic tree (HMMER, Wheeler & Eddy, 2013; EPA-NG, Barbera et al., 2019; and GAPPA, Czech et al., 2020). This tree was used to make the best prediction of the missing section of the genome and the number of copies of gene families for each ASV sequence (castor R package; Louca et al., 2018). Nearest-sequenced taxon indices for each ASV were calculated to determine the quality of the inferred predicted genomes (good quality of prediction, NSTI < 2; Langille et al., 2013). Gene families for predictions were based on the enzyme commission numbering system (i.e. EC number) from the International Union of Biochemistry and Molecular Biology (IUBMB). The predicted number of copies of gene families was normalized between ASVs in all samples to account for variability in the number of these gene families and the total abundance of specific ASVs in the community. Finally, all predicted gene families were grouped to specific metabolic reactions used to infer metabolic pathways and the abundance of these for each sample (inferred from MetaCyc pathways, *MinPath*, Ye & Doak, 2009).

2.6 | Statistical analysis

The final ASV abundance per sample table was normalized to account for differences in sampling depth by calculating a modified geometric mean and estimating sample size differences which are used to correct unequal ASV abundances between both morphs (i.e. *E. radiata* and *E. brevipes*) (package DESeq2, Love et al., 2014). Singletons were removed and this normalized table was used in subsequent analyses.

Bacterial richness, diversity (Shannon-Wiener index) and evenness (Pielou index) were calculated in all samples (package PHYLOSEQ, McMurdie & Holmes, 2013) and linear mixed models (LMM) were constructed to test for differences in these alpha-diversity indices between *E. radiata* and *E. brevipes* and the possible influence of genotype as a random predictor over these indices (package lmerTest, Kuznetsova et al., 2017). Within these LMM, relationships between alpha-diversity indices and morphological traits were also included (see Table S1 for a full list of morphological traits considered for this study). For this, morphological traits were checked for multicollinearity to reduce covariate explanatory redundancy (high collinearity as variance inflation factor > 10) and were log-transformed and scaled before analyses. A stepwise model selection approach based on the Akaike information criterion (AIC) was used to determine the optimum model that only included the most relevant morphological traits (i.e. sequential replacement model selection, package MASS, Ripley et al., 2013). Multiple-factor ANCOVAs were used to infer main effects in the LMM (covariates based on model selection, Satterthwaite's method, alpha < 0.05) and REML-likelihood ratio tests to determine random effects (alpha < 0.05, package lmerTest, Kuznetsova et al., 2017). All LMM were validated by checking all assumptions of linearity, homogeneity of variance, normality and presence of influential outliers (package performance, Lüdecke et al., 2021).

Bacterial community structure was compared between *E. radiata* and *E. brevipes* using a Permutational Multivariate Analysis of Variance (PERMANOVA, alpha < 0.05, permutations = 9999, function adonis, package vegan; Oksanen et al., 2013) based on a Bray–Curtis dissimilarity matrix calculated from square-root transformed relative abundances of ASVs. We also tested for differences in dispersion of the bacterial communities between morphs using the function *betadsiper* and *permutest* in vegan (permutations = 999, alpha < 0.05, Oksanen et al., 2013) as a model validation step (Anderson, 2014). To determine which specific ASV differed between *E. radiata* and *E. brevipes*, a multivariate generalized linear model (negative-binomial GLM) was fitted to the normalized ASV table using *Mvabund* in R (Wang et al., 2012). *p*-Values were calculated using bootstrap iterations (i.e. 1000 iterations) and were adjusted for multiple testing via a Bonferroni correction. All significant ASVs were identified to a genus level and relative abundances pooled if assigned to the same genera. Only genera with >0.5% of average relative abundance across all samples were selected for further analysis. ASVs that were not identified to a specific genus were not analysed further (i.e. these constituted approx. 39% of the total significant ASV and with an average relative abundance of 11% across the whole community). Relative abundances of the selected genera were then analysed with simple linear models and one-way ANCOVA to determine differences between *Ecklonia* morphs and the influence of morphological traits found to be relevant predictors of bacterial community composition (package car, Fox & Weisberg, 2018 and package performance, Lüdecke et al., 2021 for model validation).

To further test the hypothesis that bacterial community dissimilarity would be lowest among identical clones of *E. brevipes* compared to different unique clonal genotypes of *E. brevipes* or unique non-clonal *E. radiata* genotypes, the Bray–Curtis dissimilarities between pairs of samples in the following categories were calculated: (i) among individuals with identical clonal genotype produced by the vegetative morph, *E. brevipes* (clonal-brevipes, 'CB'; $n = 4$ possible combinations based on four clonal genotypes that had two replicates each); (ii) among different clonal genotypes of *E. brevipes* (non-clonal brevipes, 'NCB'; $n = 36$); (iii) among unique non-clonal genotypes of the sexual morph, *E. radiata* (sexual radiata, 'SR'; $n = 105$); and (iv) dissimilarities between unique non-clonal genotypes *E. radiata* and unique *E. brevipes* clonal genotypes ('SR_NCB'; $n = 135$). A univariate linear model and a one-way ANOVA were done to test for differences in the level of dissimilarity among the four categories (R Core Team, 2021, package car, Fox & Weisberg, 2018 and package PERFORMANCE, Lüdecke et al., 2021 for model validation). Contrasts between established categories were done using estimated marginal means (i.e. least-square means) and *p*-values corrected for multiple testing through a Bonferroni adjustment (package emmeans, Lenth et al., 2019). An unbalanced design with large differences in sample size among these categories limits the analysis above so, to try to account for this limitation, two subsets of Bray–Curtis distances from the above dataset were randomly selected from each established category. Random subset 1 included all categories in a balanced design based on the lowest possible sample size ($n = 4$) and random subset 2 included an unbalanced design with the same sample size for groups NCB, SR and SR_NCB ($n = 36$) and the maximum sample size for CB ($n = 4$). A similar univariate analysis as above was done for each of the random subsets.

A distance-based redundancy analysis (dbRDA) constructed from a Bray–Curtis distance matrix and the morphological traits was done to examine and visualize differences in bacterial community structure and the influence of these traits on the two *Ecklonia* morphs. For this analysis, morphological traits were also included as relevant covariates upon an initial stepwise model selection (i.e. based on AIC, package vegan, Oksanen et al., 2013). As above, all morphological traits were log-transformed, normalized (i.e. centred by mean and standard deviation, function *scale*, base R) and checked for multicollinearity before the analysis. Marginal tests (i.e. distance-based linear modelling) were done to estimate the independent influence of each morphological trait in explaining the observed variation in bacterial community structure between the two morphs (alpha < 0.05, package vegan, Oksanen et al., 2013). In addition to the dbRDA, a principal component analysis (PCA) was used to exclusively visualize the influence of morphological traits to differentiate the two morphs.

A similar statistical approach as above was used to determine functional differences (i.e. PICRUST2 predicted functional profiles) between *E. radiata* and *E. brevipes* and to test for differences in community dissimilarity among the four categories above (i.e. CB, NCB, SR and SR_NCB).

3 | RESULTS

3.1 | Influence of host genotype on associated bacterial composition and predicted function

A total of 5486 bacterial ASV were identified and remained after pre-processing (i.e. singleton removal and normalization) and used for further analysis (86% of ASV remained and 89% of all total reads retained from the original ASV abundance table, see Table S10).

Comparisons of Bray–Curtis dissimilarities between pairs of samples within the four categories of host genotype combinations showed a higher bacterial compositional dissimilarity between different morphs (SR_NCB) than among unique genotypes within each morph (NCB and SR) or among identical clones of *E. brevipes* (CB) (Figure 3a and Table S2A, $F = 24.2$, df = 3 and $p < .001$). Interestingly, compositional variability of bacterial communities was also found to be lower between individuals with identical clonal genotype (CB) compared to categories that included comparisons among individuals with different genotypes (Figure 1a, NCB, SR and SR_NCB). Additional tests with random subsets with the lowest possible balanced design ($n = 4$) and a subset adjusted to the next lowest sample size ($n = 36$) provided further evidence of these patterns despite the differing sample size (Figure S1A,B and Table S2B,C, subset 1: $F = 5.44$, df = 3 and $p = .013$; and subset 2: $F = 15.28$, df = 3 and $p < .001$).

Bray–Curtis dissimilarities from predicted metabolic pathways and the categories outlined above (i.e. CB, NCB, SR and SR_NCB) showed no differences in the functional profiles between the categories except between NCB and SR (Figure 3b) with higher functional profile dissimilarity within sexual morphs of *E. radiata* than non-clones of *E. brevipes* (Figure 3b and Table S3A, $F = 3.04$, df = 3 and $p = .03$). Further analysis with random subsets of balanced data as above showed no differences across the four categories (Figure S1C,D and Table S3B,C; subset 1: $F = 1.11$, $d = 3$ and $p = .38$; and subset 2: $F = 1.56$, df = 3 and $p = .20$). No difference in variability of predicted functional profiles was found between categories (Figure S6).

3.2 | Differences in bacterial communities driven by Ecklonia morphs

There was no differences in bacterial richness and evenness between the two *Ecklonia* morphs (Figure 4a,c, $F = 0.99$, df = 1 and p value = .33; $F = 4.23$, df = 1 and p value = .52, respectively) but bacterial diversity was lower in the sexual morph *E. radiata* (Figure 4b; $F = 5.05$, df = 1 and p value = .035). Evaluated morphological traits after model selection were not found to be significant predictors of alpha-diversity indices (Table S4, overall $F = 3.62$, df = 1 and $p > .07$). None of the bacterial alpha-diversity indices differed among
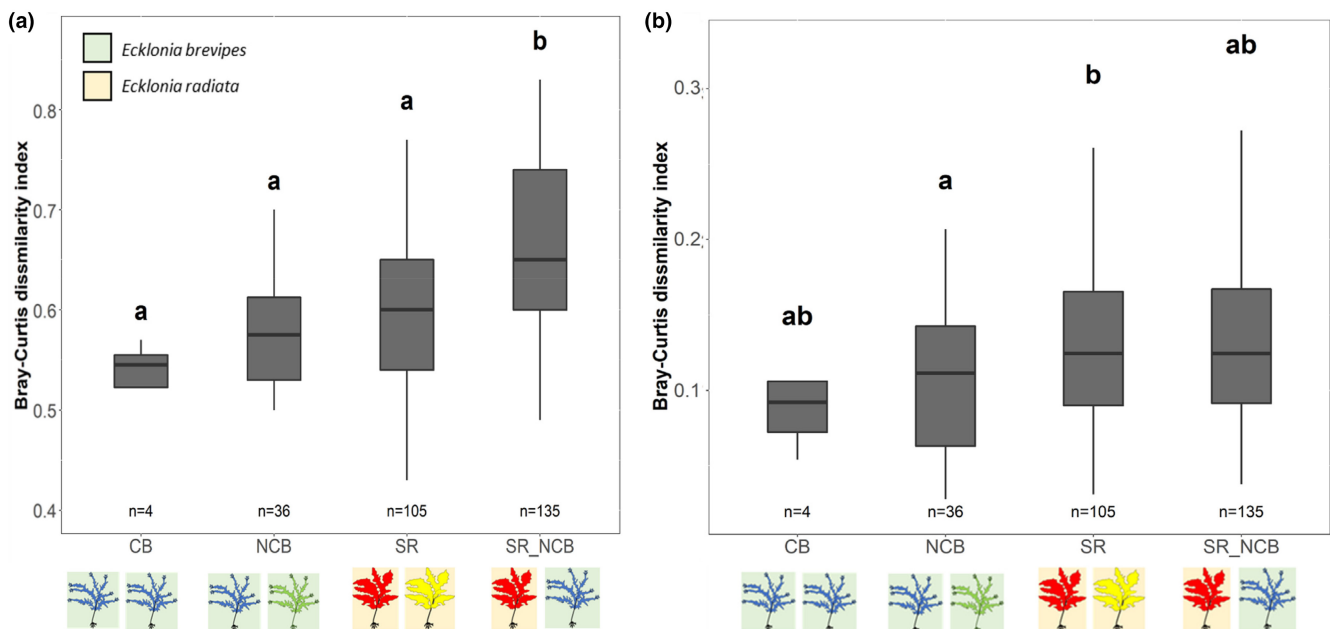

FIGURE 3 Comparison of Bray–Curtis dissimilarity distances calculated to compare (a) bacterial composition and (b) predicted metabolic pathways among established grouping categories: comparisons among individuals of the same clonal genotype of *E. brevipes* (CB, $n = 4$ clones); different clones of *E. brevipes* (NCB, $n = 36$); all individuals of *E. radiata* with unique genotypes (SR; $n = 105$) and among all genotypes of both morphs (SR_NCB; $n = 135$). Box and whisker plots show median, minimum, maximum an interquartile of the Bray–Curtis dissimilarity index per category. Different kelp colours represent different genotypes and background (green or yellow) indicates the type of *Ecklonia* morph. Significant differences across categories in a and b are denoted by different letters ($p < .05$, based on post-hoc tests and Bonferroni p-value adjustment).
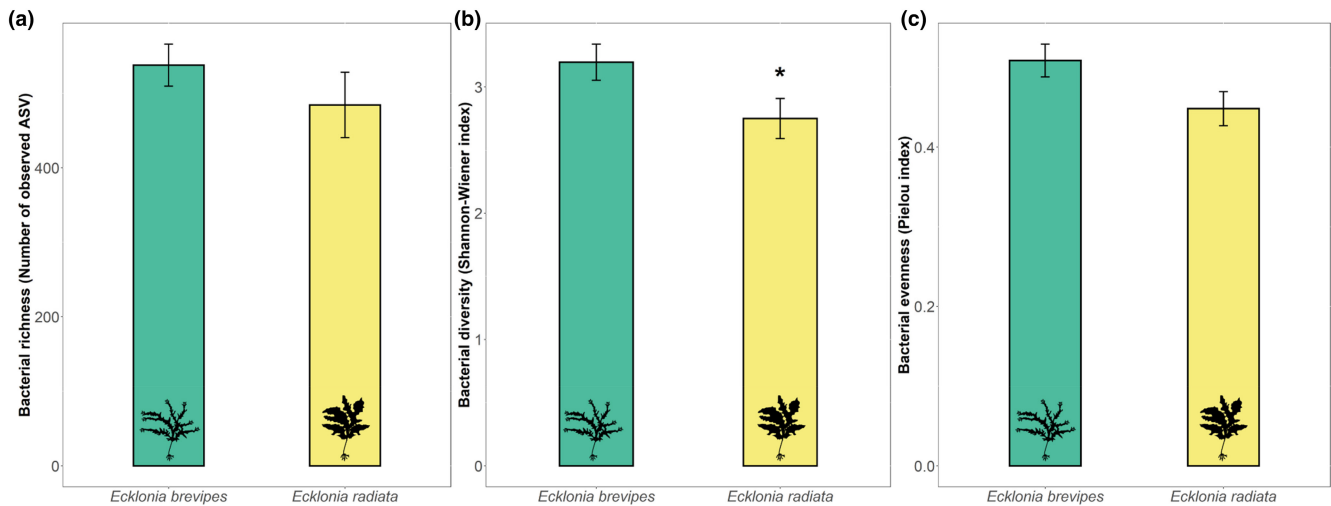
FIGURE 4 Alpha-diversity indices of host-associated bacterial communities between two Ecklonia morphs (*E. radiata* and *E. brevipes*). Significant decreases in the different alpha-diversity indices between morphs are marked with an asterisk ($p < .05$, based on the pairwise contrasts between morphs obtained from the multiple-factor ANCOVAs). These values are based on samples from 15 unique genotypes of *E. radiata* and 9 unique genotypes of E. brevipes. Values shown represent the mean ± SE of each alpha-diversity index per morph. See Table S2 for full details of statistical tests for each alpha-diversity index.
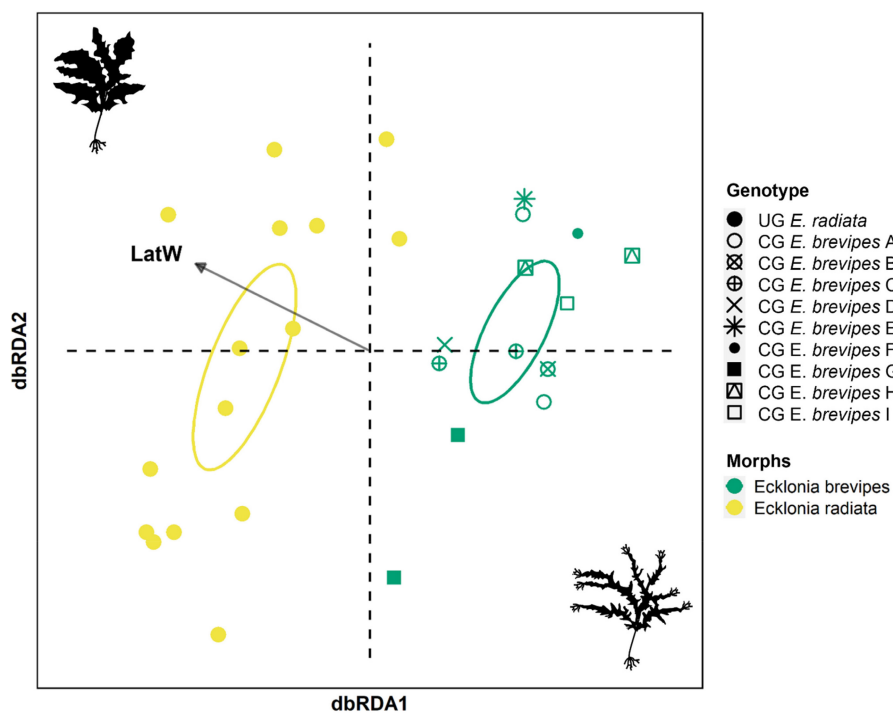

FIGURE 5 Distance-based redundancy analysis (dbRDA) and principal coordinate ordination of the differences in bacterial community composition between two morphs of Ecklonia, *E. radiata* with 15 unique genotypes (UG) and *E. brevipes* with 9 different clonal genotypes (CG). Different colours represent the two Ecklonia morphs and different shapes for *E. brevipes* show distinct clonal genotypes. All *E. radiata* genotypes were unique and are represented as circles. Ellipses represent standard error of weighted centroids and arrows indicate significant morphological traits (Lateral width, LatW).

genotypes of the two morphs (Table S4, overall LRT <0.003, df = 1 and $p > .90$).

PERMANOVA results (Figure 5, Figure S2 and Table S5A, $F = 5.02$, df = 1 and p-value < .005) showed clear differences in the bacterial assemblage structure between the two morphs that is not driven by

intra-group variability (PERMDISP, Figure S3 and Table S5B, $F = 0.45$, df = 1 and p value = .50). Measured morphological traits were found to differentiate the two morphs and as expected, the number of lateral haptera (Hap) was the main driver of this dissimilarity (PCA analysis, Figure S4). However, results of the dbRDA, stepwise

model selection and associated marginal tests showed none of the morphological traits (except LatW) predicted bacterial community structure (Figure 5 and Table S6A; marginal test: $F = 4.67$, df = 1 and p-value > .001).

The structural differences of bacterial communities between *E. radiata* and *E. brevipes* were driven by the relative abundance of 210 ASV within 53 identified genera. Of these, only seven genera showed a relative abundance higher than 0.5%, and only five were found to significantly differ between the two morphs (Figure 6 and Table S7, the full list of genera is shown in Table S8). The genera *Granulosiccocus* and *Blastopirellula* (class Gammaproteobacteria and Planctomycetes) were overall the most abundant taxa across all samples (see Figure S5). However, *Granulosiccocus* showed a higher abundance in *E. radiata* compared to *E. brevipes* (Figure 6, 73% higher in relative abundance, $p < .05$) while *Blastopirellula* and the genera, Litorimonas, Sva096 marine group and *Rubidimonas* (classes, Bacteroidia, Acidimicrobiia and Alphaproteobacteria, respectively) had greater relative abundance in *E. brevipes* (Figure 3, $p < .05$). The relative abundances of these genera showed no significant linear relationship with lateral width (Table S7, overall $F < 1.93$, df = 1 and $p > .2$).

The relative abundance of predicted bacterial metabolic pathway composition differed between the two morphs (Figure 7, PERMANOVA: $F = 4.78$, df = 1 and $p = .012$, Table S5). These differences were not driven by intra-group dispersion (Figure S6 and Table S5, $F = 1.21$, df = 1 and $p = .26$) but marginal tests of relevant morphological traits based on model selection showed the influence of lamina width (LamW) as a potential driver of predicted bacterial metabolic composition (Figure 5 and Table S6B). However, only one predicted metabolic pathway was found to differ between *Ecklonia* morphs which corresponded to a carbohydrate degradation pathway (i.e. L-rhamnose degradation, $W = 16.62$ and $p = .043$) which is 40% higher in *E. brevipes* than *E. radiata* but was an overall rare pathway (0.02% of all predicted gene families across all samples; Table S9).

4 | DISCUSSION

Host genotype is known to be an important driver of associated microbiomes through multiple mechanisms that are only beginning to be studied in marine habitat-forming species (e.g. Griffiths et al., 2019; Lachnit et al., 2009; Longford et al., 2019). Morphological variability in the host is an important factor that determines the colonization and structure of associated microbial communities (Van der Loos et al., 2019) as these differences may contribute to varying levels of resource availability and protection towards the changing environment (Dittami et al., 2021; Egan et al., 2013; Jiang et al., 2020; Whipps et al., 2008). Differences in morphological traits between individuals of a same species are undoubtedly regulated by a genetic background and influence associated microbiomes; however, other process determined by the host genotype may also be involved in shaping microbial assemblages but are yet to be clearly defined and remain challenging to study. To disentangle the roles of host

genotype independently from morphological traits, we explored variation in microbial communities between co-occurring clonal vegetative and non-clonal sexual morphs of the kelp, *E. radiata* that live interspersed on the same reefs and hence experience consistent environmental conditions.

4.1 | Genotype as a driver of bacterial assemblages on *Ecklonia radiata*

Genetic host variants and specific gene polymorphisms have been directly linked to the increase and decrease in specific bacterial groups in many host systems (Imhann et al., 2018; Wang et al., 2018). From these studies, it becomes clear that genetic variation, even between individuals in the same population, can be highly specific and, in turn, can determine individual differences in the associated microbiomes and the functions they regulate. Our results highlight the importance of the genotype in defining the associated bacterial community of *E. radiata*. Within this species, unique non-clonal sexual *E. radiata* genotypes (15 unique genotypes) and 9 unique vegetative *E. brevipes* genotypes (each with 1 or 2 identical clonal replicates) were found. Individuals within each *E. brevipes* clone genotype had a more similar and less variable bacterial composition compared to different non-clonal genotypes of *E. brevipes* and all individuals with unique genotypes of *E. radiata* that were produced sexually (Figure 1a and subset analysis in Figure S1A,B) providing evidence that host genotype plays a role in determining the microbiome. This, however, was not reflected in the functional metabolic profiles (Figure 1b and random subset analysis in Figure S1C,D) where predicted metabolic composition was found to be less variable and more similar across the different genotype categories (i.e. CB, NCB, SR and SR_NCB) than that of the same categories (Figure 1a).

With an identical genetic relatedness among individuals within clones of *E. brevipes*, it is possible that regulation of multiple processes would result in a more similar bacterial assemblage. Such processes may include epithelial release of multiple primary and secondary metabolites that influence resource allocation and availability for the microbiome (Coyte et al., 2015). This metabolite production can also control associated microbial abundances through the release of antimicrobial compounds (Kelman et al., 2001) or by regulating the host's immune response and defence to environmental change, xenobiotics or external pathogens (Chi et al., 2018; Jani & Briggs, 2018; Leopold & Busby, 2020; McKnite et al., 2012; Parkinson et al., 2015). Evidence of the importance of genetic relatedness on the regulation of functional processes that directly affect the associated microbiome can be found in many species. For example, gut microbiota from identical twins has been observed to be more similar in composition compared to fraternal twins (Goodrich et al., 2016; Selber-Hnatiw et al., 2020; Xie et al., 2016) and even determine their functional response during disease (e.g. IBD, Imhann et al., 2018). Another example in birds demonstrates that members of the same family have a more similar skin microbiome in contrast to other families of the same species (Engel et al., 2020). It is important
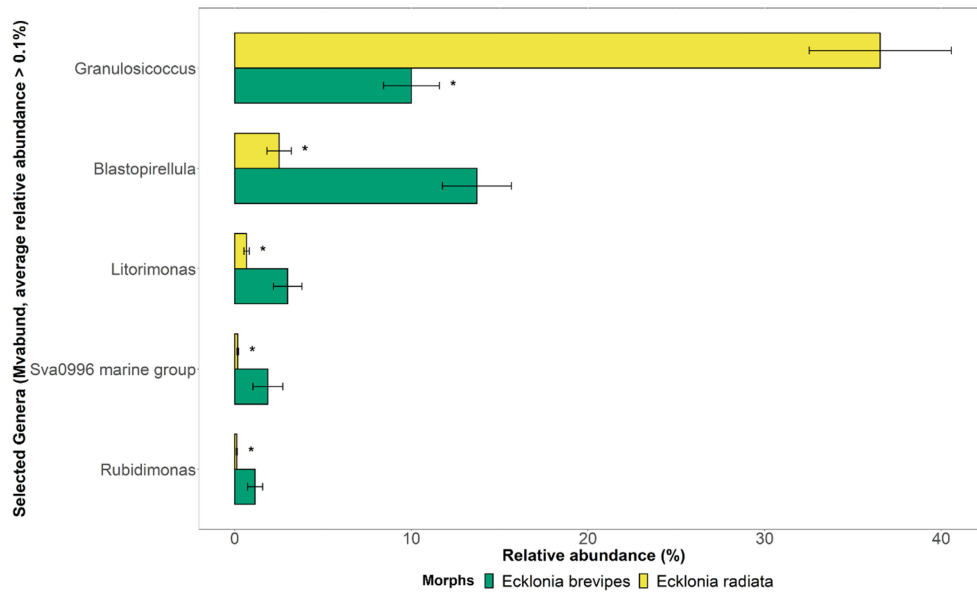
FIGURE 6 Selected genera (relative abundance >0.5%) that differed significantly between two Ecklonia morphs (*E. radiata* and *E. brevipes*, $p < .05$). Relative abundance values are shown as mean $\pm$ SE and significantly lower relative abundance between the two morphs are shown with an asterisk ($p < .05$, based on pairwise contrast obtained through a one-way ANCOVA for each genus).
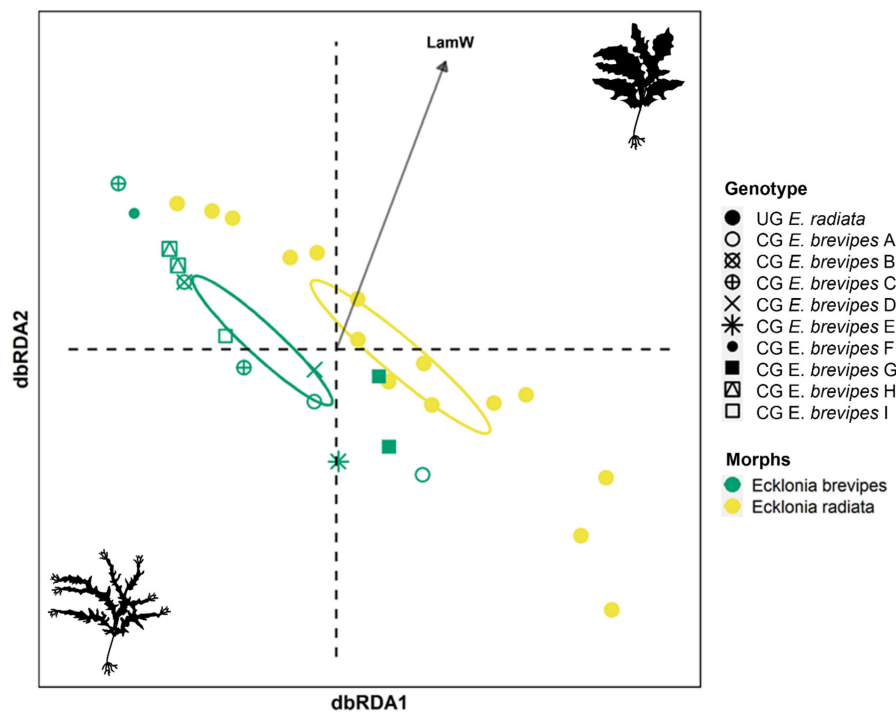

FIGURE 7 Distance-based redundancy analysis (dbRDA) and principal coordinate ordination of the compositional differences of predicted bacterial metabolic pathways composition between two morphs of *Ecklonia*, *E. radiata* with 15 unique genotypes (UG) and *E. brevipes* with 9 different clonal genotypes (CG). Different colours represent the two Ecklonia morphs and different shapes for E. brevipes show distinct clonal genotypes. All *E. radiata* genotypes were unique and are represented as circles. Ellipses represent standard error of weighted centroids and arrows indicate significant morphological traits (Lamina width, LamW).

to note that compositional and structural taxonomical differences in microbial communities between individuals may not translate to functional shifts as predicted in the present study. Large redundancy in functional roles exists across bacterial taxa (Doolittle &

Booth, 2017; Louca et al., 2018) so additional research is needed to elucidate which processes are being directly regulated by the genotypic identity of *E. radiata* individuals that possibly gives them a structural and functional genotype-specific microbiome profile.

4.2 | Morphological traits as drivers of microbiomes in two *Ecklonia radiata* morphs

Morphology is a key component that determines intraspecific variation and is directly influenced by the different genotypes present in a population. Variation in morphological traits has been seen to directly affect multiple ecosystem processes and resistance to stressors (e.g. Séguin et al., 2014; Vadillo Gonzalez et al., 2021) so it was hypothesized that morphological variability would also play a role to shape host associated microbiomes. However, its role as the main driver of microbial communities is not fully understood and other explanatory factors also regulated by the host's genotype were expected to be at play (e.g. production of secondary metabolites, immune responses or nutrient allocation). In this study, most morphological traits did not explain most variation in the structure of the host microbiome, except the presence of haptera. Although the kelp region targeted for microbial sampling was not the haptera, and was consistent across individual kelp, this is the main morphological feature that differs between morphs. Thus, any observed difference in microbial assemblage structure between morphs is very likely to be related with differences in the lateral haptera even though microbial samples were sampled consistently on similar sections of blades. Alternatively, haptera, as being vegetative-reproductive structures that have constant growth, may hold a unique localized microbial community that may be transferred to the new clone but targeted sampling on this section of the thallus is needed to assess this (Coleman & Wernberg, 2018). Kelp need high translocation of nutrients from other regions of the lamina (also seen in other Laminariales such as *Macrocystis pyrifera*, Lobban, 1978) and may provide a larger exchange surface for biofilm formation and nutrient exchange with the bacterial communities. Thus, it may be possible but still largely speculative that the quality and number of resources allocated to production of lateral haptera may modulate not only a slightly more diverse bacterial community in *E. brevipes* as seen in this study (14% more diverse than *E. radiata*), but also the specific taxa and their assembly. Additionally, a greater morphological complexity given by the haptera can directly affect the host's physicochemical properties with the formation of microniches where the microbial communities can survive and thrive (Phelps et al., 2021; Tang et al., 2010). For other kelp species, higher morphological complexity increases surface area for the establishment of heterotrophic microbial communities and biofilm formation (Van der Loos et al., 2019). Biofilm formation is directly dependent on the spatial region within individual algae as some parts of the host (i.e. haptera) may provide a better microhabitat for specific microbes (Lemay et al., 2021).

In *E. radiata*, the most abundant bacterial taxa, *Granulosiccocus*, showed a decrease in *E. brevipes* while the rest of the identified genera (*Blastopirellula*, *Litorimonas*, *Sva0996 marine group* and *Rubidomonas*) presented an increase in the latter morph. All these genera are known to be widespread in marine environments (Gonzalez et al., 2021) and appear as heterotrophic bacteria utilizing secreted nutrients from the surfaces of laminarian brown algae (Behera et al., 2017; Bengtsson & Øvreås, 2010; Park et al., 2014; Ramírez-Puebla et al., 2022; Rizzo

et al., 2016). However, *Granulosiccocus* has been seen in some studies to be more abundant in mature blades compared to newer regions with possibly higher growth rates (seen in the kelp, *Nerocystis luekeana*; Weigel & Pfister, 2021). These characteristics may provide evidence that lateral haptera and associated structures in *E. brevipes* could delimit the bacterial composition through a microhabitat that selects for specific taxa and population reduction of others. However, it is likely that even with these clear differences in bacterial composition between the two morphs, a high functional redundancy may exist.

By predicting functional abundances of genetic families using the 16S amplicon sequences, it was possible to infer a potential overview of the bacterial metabolic capacity of each associated microbiome in both *Ecklonia* morphs. Results show some evidence of different predicted functional compositions between both *Ecklonia* morphs; however, these differences are only represented significantly by a single and low abundant metabolic pathway (i.e. L-rhamnose degradation). L-rhamnose is a known sugar that appears in many carbohydrates like Pectin and Ulvan and are an important structural component in many macroalgal cell walls (Martin et al., 2014). Many known bacterial taxa can degrade not only L-rhamnose but many other sugars available in macroalgal laminar surfaces (Martin et al., 2014); therefore, the relatively higher levels of this potential metabolic activity in *E. brevipes* may not reflect a substantial difference in the functional roles of the associated microbiomes. Some examples in marine organisms are known where large taxonomical differences in microbial communities exist between individuals of the same species but do not translate to differences in the functional metabolic processes they regulate (e.g. *Ulva australis*, Burke et al., 2011 or sponges, Thomas et al., 2016). Results in this study may suggest a possible functional redundancy between bacterial communities that is uncoupled to the observed differences in bacterial community composition and structure between both *Ecklonia* morphs. It needs to be noted that the prediction of functional profiles and other annotation methods such as the one used in this study have important limitations when interpreting functions in microbial communities. For example, functional predictions can be highly variable compared to data obtained through direct functional assessments such as shotgun metagenomic sequencing and transcriptomics (Toole et al., 2021) and may be poorly represented in non-human environments (Sun et al., 2020). Nonetheless, the available genomes from which the present functional profiles are being predicted are in constant development and enough resolution at this stage exists to be able to do a general metabolic profiling of the bacterial communities (Douglas et al., 2020; Trego et al., 2022). Thus, the results here can provide a rough understanding of the functional capacity of the kelp's associated bacterial community, but further research should be done to assess specific functions and real-time intraspecific genetic regulation that could vary between the two morphs.

In this study, clear differences in bacterial communities were observed between two different morphological groups (*E. radiata* and *E. brevipes*) but also at the level of individuals with distinct genotype. Specifically, individuals of the same clonal genotype of *E. brevipes*

show evidence of a more similar bacterial community composition and possibly a functional profile that may not be completely defined by morphological traits or the environment. Although a limitation of this study was a low number of unique clones ($n = 4$ clonal genotypes with 2 individuals each), we show using random subsets with varying and balanced sample sizes, that there is still a higher similarity in bacterial communities among individuals within each clone of *E. brevipes* compared to all unique genotypes of *E. radiata*. Genetic relatedness is thus strongly associated with microbial communities in kelps, but further research is needed to corroborate this finding. A deeper understanding of the mechanisms and processes that host genotype regulates within these systems will expand the knowledge of holobionts within a constantly deteriorating environment, but also inform of the potential of specific genotypes on increasing the performance of macroalgae restoration (Qiu et al., 2019; Wood et al., 2021) or for commercial use.

CONFLICT OF INTEREST STATEMENT

The authors declare that they have no conflicts of interest that could influence the work within this study.

DATA AVAILABILITY STATEMENT

Bacterial raw amplicon sequence reads were deposited in the SRA (BioProject: PRJNA891085) with corresponding metadata based on the respective SRA submission, using the MIMARKS Survey related MIxS package for 16S amplicon sequencing. Genetic datasets for *E. radiata* are deposited on DRYAD at https://doi.org/10.5061/dryad.fn2z34ttg and for *E. brevipes* on Figshare (https://doi.org/10.6084/m9.figshare.19772866.v1).

BENEFIT-SHARING STATEMENTS

The present research collaboration was developed with scientists from different states and institutions in Australia (NSW and WA) through an exchange of data and ideas that ultimately culminated in this manuscript. Amplicon and Genomic data were provided from samples in WA and a formal analysis (e.g. molecular, bioinformatic and statistical) was conducted in NSW. All collaborators are included as co-authors and all data have been publicly shared to the broader scientific community as mentioned above.

ORCID

Sebastian Vadillo Gonzalez https://orcid.org/0000-0002-3710-0406
Sofie Vranken https://orcid.org/0000-0002-8459-041X
Ezequiel M. Marzinelli https://orcid.org/0000-0002-3762-3389

REFERENCES

Anderson, M. J. (2014). Permutational multivariate analysis of variance (PERMANOVA). *Wiley Statsref: Statistics Reference Online*, 1–15 https://doi.org/10.1002/9781118445112.stat07841

Barbera, P., Kozlov, A. M., Czech, L., Morel, B., Darriba, D., Flouri, T., & Stamatakis, A. (2019). EPA-ng: Massively parallel evolutionary placement of genetic sequences. *Systematic Biology*, 68(2), 365–369. https://doi.org/10.1093/sysbio/syy054

Behera, P., Mahapatra, S., Mohapatra, M., Kim, J. Y., Adhya, T. K., Raina, V., Suar, M., Pattnaik, A. K., & Rastogi, G. (2017). Salinity and macrophyte drive the biogeography of the sedimentary bacterial communities in a brackish water tropical coastal lagoon. *Science of the Total Environment*, 595, 472–485.

Bengtsson, M. M., & Øvreås, L. (2010). Planctomycetes dominate biofilms on surfaces of the kelp Laminaria hyperborea. *BMC Microbiology*, 10(1), 1–12.

Benson, A. K., Kelly, S. A., Legge, R., Ma, F., Low, S. J., Kim, J., Zhang, M., Oh, P. L., Nehrenberg, D., Hua, K., & Kachman, S. D. (2010). Individuality in gut microbiota composition is a complex polygenic trait shaped by multiple environmental and host genetic factors. *Proceedings of the National Academy of Sciences of the United States of America*, 107(44), 18933–18938.

Burke, C., Steinberg, P., Rusch, D., Kjelleberg, S., & Thomas, T. (2011). Bacterial community assembly based on functional genes rather than species. *Proceedings of the National Academy of Sciences of the United States of America*, 108(34), 14288–14293.

Callahan, B. J., McMurdie, P. J., Rosen, M. J., Han, A. W., Johnson, A. J. A., & Holmes, S. P. (2016). DADA2: High-resolution sample inference from Illumina amplicon data. *Nature Methods*, 13(7), 581–583.

Catchen, J., Hohenlohe, P. A., Bassham, S., Amores, A., & Cresko, W. A. (2013). Stacks: An analysis tool set for population genomics. *Molecular Ecology*, 22(11), 3124–3140.

Chi, L., Gao, B., Tu, P., Liu, C. W., Xue, J., Lai, Y., Ru, H., & Lu, K. (2018). Individual susceptibility to arsenic-induced diseases: The role of host genetics, nutritional status, and the gut microbiome. *Mammalian Genome*, 29(1), 63–79.

Coleman, M. A., & Wernberg, T. (2018). Genetic and morphological diversity in sympatric kelps with contrasting reproductive strategies. *Aquatic Biology*, 27, 65–73.

Coyte, K. Z., Schluter, J., & Foster, K. R. (2015). The ecology of the microbiome: Networks, competition, and stability. *Science*, *350*(6261), 663–666.

Czech, L., Barbera, P., & Stamatakis, A. (2020). Genesis and Gappa: Processing, analyzing and visualizing phylogenetic (placement) data. *Bioinformatics*, *36*(10), 3263–3265.

Danecek, P., Auton, A., Abecasis, G., Albers, C. A., Banks, E., DePristo, M. A., Handsaker, R. E., Lunter, G., Marth, G. T., Sherry, S. T., & McVean, G. (2011). The variant call format and VCFtools. *Bioinformatics*, *27*(15), 2156–2158.

DeWeese, K. J., & Osborne, M. G. (2021). Understanding the metabolome and metagenome as extended phenotypes: The next frontier in macroalgae domestication and improvement. *Journal of the World Aquaculture Society*, *52*(5), 1009–1030.

Dittami, S. M., Arboleda, E., Auguet, J. C., Bigalke, A., Briand, E., Cárdenas, P., Cardini, U., Decelle, J., Engelen, A. H., Eveillard, D., & Gachon, C. M. (2021). A community perspective on the concept of marine holobionts: Current status, challenges, and future directions. *PeerJ*, *9*, e10911.

Doolittle, W. F., & Booth, A. (2017). It's the song, not the singer: An exploration of holobiosis and evolutionary theory. *Biology and Philosophy*, *32*, 5–24.

Douglas, G. M., Maffei, V. J., Zaneveld, J. R., Yurgel, S. N., Brown, J. R., Taylor, C. M., Huttenhower, C., & Langille, M. G. (2020). PICRUSt2 for prediction of metagenome functions. *Nature Biotechnology*, *38*(6), 685–688.

Dubé, C. E., Ziegler, M., Mercière, A., Boissin, E., Planes, S., Bourmaud, C. F., & Voolstra, C. R. (2021). Naturally occurring fire coral clones demonstrate a genetic and environmental basis of microbiome composition. *Nature Communications*, *12*(1), 6402.

Egan, S., Harder, T., Burke, C., Steinberg, P., Kjelleberg, S., & Thomas, T. (2013). The seaweed holobiont: Understanding seaweed–bacteria interactions. *FEMS Microbiology Reviews*, *37*(3), 462–476.

Engel, K., Pankoke, H., Jünemann, S., Brandl, H. B., Sauer, J., Griffith, S. C., Kalinowski, J., & Caspers, B. A. (2020). Family matters: Skin microbiome reflects the social group and spatial proximity in wild zebra finches. *BMC Ecology*, *20*(1), 1–11.

Fietz, K., Hintze, C. O. R., Skovrind, M., Nielsen, T. K., Limborg, M. T., Krag, M. A., Palsbøll, P. J., Hansen, L. H., Møller, P. R., & Gilbert, M. T. P. (2018). Mind the gut: Genomic insights to population divergence and gut microbial composition of two marine keystone species. *Microbiome*, *6*(1), 1–16.

Fox, J., & Weisberg, S. (2018). Visualizing fit and lack of fit in complex regression models with predictor effect plots and partial residuals. *Journal of Statistical Software*, *87*(1), 1–27.

Glasl, B., Smith, C. E., Bourne, D. G., & Webster, N. S. (2019). Disentangling the effect of host-genotype and environment on the microbiome of the coral *Acropora tenuis*. *PeerJ*, *7*, e6377.

Gonzalez, N. B. C., Corredor, A. N. N., Kleine, L. L., & Castaño, D. M. (2021). Temporal changes of the epiphytic bacteria community from the marine macroalga *Ulva lactuca* (Santa Marta, Colombian-Caribbean). *Current Microbiology*, *78*(2), 534–543.

Goodrich, J. K., Davenport, E. R., Beaumont, M., Jackson, M. A., Knight, R., Ober, C., Spector, T. D., Bell, J. T., Clark, A. G., & Ley, R. E. (2016). Genetic determinants of the gut microbiome in UK twins. *Cell Host & Microbe*, *19*(5), 731–743.

Griffiths, S. M., Antwis, R. E., Lenzi, L., Lucaci, A., Behringer, D. C., Butler, M. J., IV, & Preziosi, R. F. (2019). Host genetics and geography influence microbiome composition in the sponge *Ircinia campana*. *Journal of Animal Ecology*, *88*(11), 1684–1695.

Griffiths, S. M., Harrison, X. A., Weldon, C., Wood, M. D., Pretorius, A., Hopkins, K., Fox, G., Preziosi, R. F., & Antwis, R. E. (2018). Genetic variability and ontogeny predict microbiome structure in a disease-challenged montane amphibian. *The ISME Journal*, *12*(10), 2506–2517.

Hayashi, Y., Notoya, M., & Yotsukura, N. (2020). Abnormal asexual reproduction of thalli of *Ecklonia stolonifera* (Laminariales, Phaeophyceae) off the coast of Nakanoshima in the Oki Islands, Japan. *Botanica Marina*, *63*(3), 247–252.

Imhann, F., Vila, A. V., Bonder, M. J., Fu, J., Gevers, D., Visschedijk, M. C., Spekhorst, L. M., Alberts, R., Franke, L., van Dullemen, H. M., & Ter Steege, R. W. (2018). Interplay of host genetics and gut microbiota underlying the onset and clinical presentation of inflammatory bowel disease. *Gut*, *67*(1), 108–119.

Jani, A. J., & Briggs, C. J. (2018). Host and aquatic environment shape the amphibian skin microbiome but effects on downstream resistance to the pathogen *Batrachochytrium dendrobatidis* are variable. *Frontiers in Microbiology*, *9*, 487.

Jiang, H., Chen, W., Su, L., Huang, M., Lin, L., Su, Q., Li, G., Ahmad, H. I., Li, L., Zhang, X., & Li, H. (2020). Impact of host intraspecies genetic variation, diet, and age on bacterial and fungal intestinal microbiota in tigers. *MicrobiologyOpen*, *9*(7), e1050.

Kamvar, Z. N., Brooks, J. C., & Grünwald, N. J. (2015). Novel R tools for analysis of genome-wide population genetic data with emphasis on clonality. *Frontiers in Genetics*, *6*, 208.

Kamvar, Z. N., Tabima, J. F., & Grünwald, N. J. (2014). Poppr: An R package for genetic analysis of populations with clonal, partially clonal, and/or sexual reproduction. *PeerJ*, *2*, e281.

Kelman, D., Kashman, Y., Rosenberg, E., Ilan, M., Ifrach, I., & Loya, Y. (2001). Antimicrobial activity of the reef sponge *Amphimedon viridis* from the Red Sea: Evidence for selective toxicity. *Aquatic Microbial Ecology*, *24*(1), 9–16.

Kirkman, H. (1981). The first year in the life history and the survival of the juvenile marine macrophyte, *Ecklonia radiata* (Turn.) J. Agardh. *Journal of Experimental Marine Biology and Ecology*, *55*(2–3), 243–254.

Klindworth, A., Pruesse, E., Schweer, T., Peplies, J., Quast, C., Horn, M., & Glöckner, F. O. (2013). Evaluation of general 16S ribosomal RNA gene PCR primers for classical and next-generation sequencing-based diversity studies. *Nucleic Acids Research*, *41*(1), e1.

Kuznetsova, A., Brockhoff, P. B., & Christensen, R. H. (2017). lmerTest package: Tests in linear mixed effects models. *Journal of Statistical Software*, *82*, 1–26.

Lachnit, T., Wahl, M., & Harder, T. (2009). Isolated thallus-associated compounds from the macroalga *Fucus vesiculosus* mediate bacterial surface colonization in the field similar to that on the natural alga. *Biofouling*, *26*(3), 247–255.

Langille, M. G., Zaneveld, J., Caporaso, J. G., McDonald, D., Knights, D., Reyes, J. A., Clemente, J. C., Burkepile, D. E., Thurber, R. L. V., Knight, R., & Beiko, R. G. (2013). Predictive functional profiling of microbial communities using 16S rRNA marker gene sequences. *Nature Biotechnology*, *31*(9), 814–821.

Lemay, M. A., Davis, K. M., Martone, P. T., & Parfrey, L. W. (2021). Kelp-associated microbiota are structured by host anatomy. *Journal of Phycology*, *57*(4), 1119–1130.

Lenth, R., Singmann, H., Love, J., Buerkner, P., & Herve, M. (2019). *Package 'emmeans'*.

Leopold, D. R., & Busby, P. E. (2020). Host genotype and colonist arrival order jointly govern plant microbiome composition and function. *Current Biology*, *30*(16), 3260–3266.

Lobban, C. S. (1978). Translocation of 14C in *Macrocystis pyrifera* (giant kelp). *Plant Physiology*, *61*(4), 585–589.

Longford, S. R., Campbell, A. H., Nielsen, S., Case, R. J., Kjelleberg, S., & Steinberg, P. D. (2019). Interactions within the microbiome alter microbial interactions with host chemical defences and affect disease in a marine holobiont. *Scientific Reports*, *9*(1), 1–13.

Louca, S., Polz, M. F., Mazel, F., Albright, M. B., Huber, J. A., O'Connor, M., Ackermann, M., Hanhn, A. S., Srivastava, D. S., Crowe, S. A., Doebeli, M., & Parfrey, L. W. (2018). Function and functional redundancy in microbial systems. *Nature Ecology & Evolution*, *2*(6), 936–943.

Love, M. I., Huber, W., & Anders, S. (2014). Moderated estimation of fold change and dispersion for RNA-seq data with DESeq2. *Genome Biology*, *15*(12), 1–21.

Lüdecke, D., Ben-Shachar, M. S., Patil, I., Waggoner, P., & Makowski, D. (2021). performance: An R package for assessment, comparison and testing of statistical models. *Journal of Open Source Software*, *6*(60), 3139.

Martin, M. (2011). Cutadapt removes adapter sequences from high-throughput sequencing reads. *EMBnet.journal*, *17*(1), 10–12.

Martin, S., Portetelle, D., Michel, G., & Vandenbol, M. (2014). Microorganisms living on macroalgae: Diversity, interactions, and biotechnological applications. *Applied Microbiology and Biotechnology*, *98*(7), 2917–2935. https://doi.org/10.1007/s00253-014-5557-2

Marzinelli, E. M., Campbell, A. H., Zozaya Valdes, E., Vergés, A., Nielsen, S., Wernberg, T., De Bettignies, T., Bennett, S., Caporaso, J. G., Thomas, T., & Steinberg, P. D. (2015). Continental-scale variation in seaweed host-associated bacterial communities is a function of host condition, not geography. *Environmental Microbiology*, *17*(10), 4078–4088.

McKnite, A. M., Perez-Munoz, M. E., Lu, L., Williams, E. G., Brewer, S., Andreux, P. A., Bastiaansen, J. W., Wang, X., Kachman, S. D., Auwerx, J., & Williams, R. W. (2012). Murine gut microbiota is defined by host genetics and modulates variation of metabolic traits. *PLoS One*, *7*(6), e39191.

McMurdie, P. J., & Holmes, S. (2013). phyloseq: An R package for reproducible interactive analysis and graphics of microbiome census data. *PLoS One*, *8*(4), e61217.

Oksanen, J., Blanchet, F. G., Kindt, R., Legendre, P., Minchin, P. R., O'hara, R. B., Simpson, G. L., Solymos, P., Stevens, M. H. H., Wagner, H., & Oksanen, M. J. (2013). *Package 'vegan'*. Community ecology package, version, 2(9), 1–295.

Park, S., Jung, Y. T., Won, S. M., Park, J. M., & Yoon, J. H. (2014). *Granulosicoccus undariae* sp. nov., a member of the family Granulosicoccaceae isolated from a brown algae reservoir and emended description of the genus *Granulosicoccus*. *Antonie Van Leeuwenhoek*, *106*(5), 845–852.

Parkinson, J. E., Banaszak, A. T., Altman, N. S., LaJeunesse, T. C., & Baums, I. B. (2015). Intraspecific diversity among partners drives functional variation in coral symbioses. *Scientific Reports*, *5*(1), 1–12.

Pearce, D. S., Hoover, B. A., Jennings, S., Nevitt, G. A., & Docherty, K. M. (2017). Morphological and genetic factors shape the microbiome of a seabird species (*Oceanodroma leucorhoa*) more than environmental and social factors. *Microbiome*, *5*(1), 1–16.

Phelps, C. M., McMahon, K., Bissett, A., Bernasconi, R., Steinberg, P. D., Thomas, T., Marzinelli, E. M., & Huggett, M. J. (2021). The surface bacterial community of an Australian kelp shows cross-continental variation and relative stability within regions. *FEMS Microbiology Ecology*, *97*(7), fiab089.

Qiu, Z., Coleman, M. A., Provost, E., Campbell, A. H., Kelaher, B. P., Dalton, S. J., Thomas, T., Steinberg, P. D., & Marzinelli, E. M. (2019). Future climate change is predicted to affect the microbiome and condition of habitat-forming kelp. *Proceedings of the Royal Society B: Biological Sciences*, *286*(1896), 20181887.

Quast, C., Pruesse, E., Yilmaz, P., Gerken, J., Schweer, T., Yarza, P., Peplies, J., & Glöckner, F. O. (2012). The SILVA ribosomal RNA gene database project: Improved data processing and web-based tools. *Nucleic Acids Research*, *41*(D1), D590–D596.

Ramírez-Puebla, S. T., Weigel, B. L., Jack, L., Schlundt, C., Pfister, C. A., & Mark Welch, J. L. (2022). Spatial organization of the kelp microbiome at micron scales. *Microbiome*, *10*(1), 1–20.

Ripley, B., Venables, B., Bates, D. M., Hornik, K., Gebhardt, A., Firth, D., & Ripley, M. B. (2013). *Package 'mass'*. Cran r, 538, 113–120.

Rizzo, L., Fraschetti, S., Alifano, P., Pizzolante, G., & Stabili, L. (2016). The alien species *Caulerpa cylindracea* and its associated bacteria in the Mediterranean Sea. *Marine Biology*, *163*(1), 4.

Rosenberg, E., & Zilber-Rosenberg, I. (2014). *The hologenome concept: Human, animal and plant microbiota*. Springer Science & Business Media.

Rothman, M. D., Mattio, L., Wernberg, T., Anderson, R. J., Uwai, S., Mohring, M. B., & Bolton, J. J. (2015). A molecular investigation of the genus *Ecklonia* (Phaeophyceae, Laminariales) with special focus on the Southern Hemisphere. *Journal of Phycology*, *51*(2), 236–246.

Sallinger, E., Robeson, M. S., & Haselkorn, T. S. (2021). Characterization of the bacterial microbiomes of social amoebae and exploration of the roles of host and environment on microbiome composition. *Environmental Microbiology*, *23*(1), 126–142.

Séguin, A., Harvey, É., Archambault, P., Nozais, C., & Gravel, D. (2014). Body size as a predictor of species loss effect on ecosystem functioning. *Scientific Reports*, *4*(1), 1–5.

Selber-Hnatiw, S., Sultana, T., Tse, W., Abdollahi, N., Abdullah, S., Al Rahbani, J., Alazar, D., Alrumhein, N. J., Aprikian, S., Arshad, R., & Azuelos, J. D. (2020). Metabolic networks of the human gut microbiota. *Microbiology*, *166*(2), 96–119.

Severn-Ellis, A. A., Scheben, A., Neik, T. X., Saad, N. S. M., Pradhan, A., & Batley, J. (2020). Genotyping for species identification and diversity assessment using double-digest restriction site-associated DNA sequencing (ddRAD-seq). In M. Jain & R. Garg (Eds.), *Legume genomics: Methods and protocols* (Vol. *2107*, pp. 159–187). Humana. https://doi.org/10.1007/978-1-0716-0235-5_8

Sun, S., Jones, R. B., & Fodor, A. A. (2020). Inference-based accuracy of metagenome prediction tools varies across sample types and functional categories. *Microbiome*, *8*(1), 1–9.

Tang, K. W., Turk, V., & Grossart, H. P. (2010). Linkage between crustacean zooplankton and aquatic bacteria. *Aquatic Microbial Ecology*, *61*(3), 261–277.

Thomas, T., Moitinho-Silva, L., Lurgi, M., Björk, J. R., Easson, C., Astudillo-García, C., Olson, J. B., Erwin, P. M., Lopez-Legentil, S., Luter, H., Chaves-Fonnegra, A., Costa, R., Schupp, P. J., Steindler, L., Erpenbeck, D., Gilbert, J., Knight, R., Ackermann, G., Lopez, J. V., ... Webster, N. S. (2016). Diversity, structure and convergent evolution of the global sponge microbiome. *Nature Communications*, *7*(1), 11870.

Toole, D. R., Zhao, J., Martens-Habbena, W., & Strauss, S. L. (2021). Bacterial functional prediction tools detect but underestimate metabolic diversity compared to shotgun metagenomics in Southwest Florida soils. *Applied Soil Ecology*, *168*, 104129.

Trego, A., Keating, C., Nzeteu, C., Graham, A., O'Flaherty, V., & Ijaz, U. Z. (2022). Beyond basic diversity estimates—Analytical tools for mechanistic interpretations of amplicon sequencing data. *Microorganisms*, *10*(10), 1961.

Uren Webster, T. M., Consuegra, S., Hitchings, M., & Garcia de Leaniz, C. (2018). Interpopulation variation in the Atlantic salmon microbiome reflects environmental and genetic diversity. *Applied and Environmental Microbiology*, *84*(16), e00691–e00618.

Vadillo Gonzalez, S., Johnston, E. L., Dafforn, K. A., O'Connor, W. A., & Gribben, P. E. (2021). Body size affects lethal and sublethal responses to organic enrichment: Evidence of associational susceptibility for an infaunal bivalve. *Marine Environmental Research*, *169*, 105391.

Van der Loos, L. M., Eriksson, B. K., & Salles, J. F. (2019). The macroalgal holobiont in a changing sea. *Trends in Microbiology*, *27*(7), 635–650.

Vranken, S., Scheben, A., Batley, J., Wernberg, T., & Coleman, M. A. (2022). Genomic consequences and selection efficacy in sympatric sexual versus asexual kelps. *Frontiers in Marine Sciences*, *9*, 921912. https://doi.org/10.3389/fmars.2022.921912

Vranken, S., Wernberg, T., Scheben, A., Severn-Ellis, A. A., Batley, J., Bayer, P. E., Edwards, D., Wheeler, D., & Coleman, M. A. (2021). Genotype–environment mismatch of kelp forests under climate change. *Molecular Ecology*, *30*(15), 3730–3746.

Wang, J., Chen, L., Zhao, N., Xu, X., Xu, Y., & Zhu, B. (2018). Of genes and microbes: Solving the intricacies in host genomes. *Protein & Cell*, *9*(5), 446–461.

Wang, Y. I., Naumann, U., Wright, S. T., & Warton, D. I. (2012). mvabund – An R package for model-based analysis of multivariate abundance data. *Methods in Ecology and Evolution*, *3*(3), 471–474.

Weigel, B. L., & Pfister, C. A. (2021). Oxygen metabolism shapes microbial settlement on photosynthetic kelp blades compared to artificial kelp substrates. *Environmental Microbiology Reports*, *13*(2), 176–184.

Wernberg, T., Coleman, M. A., Babcock, R. C., Bell, S. Y., Bolton, J. J., Connell, S. D., Hurd, C. L., Johnson, C. R., Marzinelli, E. M., Shears, N. T., & Steinberg, P. D. (2019). Biology and ecology of the globally significant kelp *Ecklonia radiata*. *Oceanography and Marine Biology*, *57*, 265–324.

Wheeler, T. J., & Eddy, S. R. (2013). nhmmer: DNA homology search with profile HMMs. *Bioinformatics*, *29*(19), 2487–2489.

Whipps, J., Hand, P., Pink, D., & Bending, G. D. (2008). Phyllosphere microbiology with special reference to diversity and plant genotype. *Journal of Applied Microbiology*, *105*(6), 1744–1755.

Wood, G., Marzinelli, E., Campbell, A., Steinberg, P., Verges, A., & Coleman, M. (2021). Using genomics to design and evaluate restoration and future-proofing of underwater forests. *Phycologia*, *60*, 32–33.

Wood, G., Steinberg, P. D., Campbell, A. H., Vergés, A., Coleman, M. A., & Marzinelli, E. M. (2022). Host genetics, phenotype and geography structure the microbiome of a foundational seaweed. *Molecular Ecology*, *31*(7), 2189–2206.

Xie, H., Guo, R., Zhong, H., Feng, Q., Lan, Z., Qin, B., Ward, K. J., Jackson, M. A., Xia, Y., Chen, X., & Chen, B. (2016). Shotgun metagenomics of 250 adult twins reveals genetic and environmental impacts on the gut microbiome. *Cell Systems*, *3*(6), 572–584.

Ye, Y., & Doak, T. G. (2009). A parsimony approach to biological pathway reconstruction/inference for genomes and metagenomes. *PLoS Computational Biology*, *5*(8), e1000465.

SUPPORTING INFORMATION

Additional supporting information can be found online in the Supporting Information section at the end of this article.

How to cite this article: Vadillo Gonzalez, S., Vranken, S., Coleman, M. A., Wernberg, T., Steinberg, P. D., & Marzinelli, E. M. (2023). Host genotype and microbiome associations in co-occurring clonal and non-clonal kelp, *Ecklonia radiata*. *Molecular Ecology*, *32*, 4584–4598. https://doi.org/10.1111/mec.17056